RESULTS OF THE PIROG 8 BALLOON FLIGHT WITH AN EMBARKED EXPERIMENT BASED ON A 425/441 GHz SIS RECEIVER FOR 0_2 SEARCH

by (alphabetical order):

A. Deschamps[1], P. Encrenaz[1], P. Febvre[1*], H.G. Florén[2], S. George[1], B. Lecomte[1], B. Ljung[3], L. Nordh[2], G. Olofsson[2], L. Pagani[1], J.R. Pardo[1], I. Peron[1], M. Sjökvist[3], K. Stegner[3], L. Stenmark[4], J. Tauber[5], and C. Ullberg[4]

[1] DEMIRM - PARIS OBSERVATORY - 75014 PARIS - FRANCE - E-mail: Pascal.Febvre@univ-savoie.fr

[2] STOCKHOLM OBSERVATORY - S-13336 SALTSJÖBADEN - SWEDEN

[3] SWEDISH SPACE CORPORATION - P.O. Box 4207 - S-17104 SOLNA - SWEDEN

[4] ACR ELECTRONIC AB - BOX 99 - 61922 TROSA - SWEDEN

[5] ESTEC - ASTROPHYSICS DIVISION - 2200 AG - NOORDWIJK - THE NETHERLANDS

CNES - AIRE-SUR-L'ADOUR - FRANCE

* New address: LAHC - UNIVERSITE DE SAVOIE - 73376 LE BOURGET DU LAC CEDEX - FRANCE

Abstract. The swedish-french PIROG 8 project (Pointed InfraRed Observation Gondola) has been developped in 1996/1997 in order to try to detect the presence of molecular oxygen in two molecular clouds of the interstellar medium: NGC7538 and W51. PIROG 8 consists of a 500 kg gondola carrying a 60 cm diameter Cassegrain telescope equipped with a 425/441 GHz SIS heterodyne receiver at its focus. This balloon-borne submillimeter SIS experiment successfully flew in september 1997 from the south-west of France. An overview of the technical experiment behaviour during flight is presented along with some performed measurements.

I - Introduction

The scientific goal of the PIROG 8 project (Pointed InfraRed Observation Gondola) was to observe simultaneously the O_2 line at 425 GHz and the ^{13}CO line at 441 GHz in the molecular clouds of the interstellar medium by heterodyne spectrometry. The main scientific interest is to detect molecular oxygen which has never been observed in the interstellar medium so far. The theoretical models predict[1] that the line emissivity is weak: about 500 mK.km.s^{-1} in dark molecular clouds. Consequently, it is necessary to use a sensitive receiver with a good spectral resolution. The simultaneous observation of the ^{13}CO line allows to verify the correct operation of the receiver and the pointing of the telescope.

In order to be free from the Earth atmosphere, the experiment must observe at high altitude so it has been embarked on the PIROG gondola, run by the Swedish Space Corporation, which flew 7 times in the past.

The heterodyne receiver developped for the PIROG 8 project consists of a sensitive front-end cooled at liquid helium temperature which feeds an autocorrelator spectrometer (back-end). The cryostat used to cool the receiver front-end operates at ambient pressure ($p \approx 3$ mbar at 39 km altitude) so that the SIS mixer is at a physical temperature of about 1.5 K. The cryostat has been provided by ESTEC along with the autocorrelator spectrometer. Both have been successfully used during former flights.

The PIROG 8 instrument has been developped at the Observatory of Paris between september 95 and june 96 in order to be ready for a flight initially scheduled for september 96 and postponed to may 97. This delay has allowed some additional tests to be performed on the instrument: in particular some tests of the receiver behaviour in the real low-pressure environment (measurements of cryostat hold time, receiver noise temperature and of physical temperature profiles of most sub-systems) have been made during winter 96 at the Observatory of Paris. The integration of the instrument on the PIROG 8 gondola took place in march 97 in Trosa (Sweden) at the ACR facility where the gondola was designed and built. Final integration including control of the receiver by the PIROG ground station has been made at the CNES balloon base in Aire-sur-l'Adour (France) during april and early may 97. Payload check and flight simulations procedures have been defined and tested during the same period. The flight, planned in may 97 has been delayed to september 97 due to bad weather conditions and balloon-flight safety regulations. Payload check procedures and flight simulations have been fine-tuned in early september

and the flight occurred on september 25th, 1997. The flight duration was 11 hours from take-off to cut-down with more than 8 hours at the ceiling altitude of about 39.5 km.

II - Technical features of the PIROG heterodyne SIS instrument

II.1. General design

The PIROG 8 receiver is based on the technology of SIS mixers. The mixer block[2] uses a reduced-height waveguide and has an integrated Potter horn[3]. It is sensitive to signals of horizontal polarization at frequencies of 425 and 441 GHz on an instantaneous bandwidth of 320 MHz. The SIS mixer uses one mechanical contacting backshort which has been fixed after proper optimization in the laboratory. It is cooled in a cryostat at liquid helium temperature, along with the HEMT amplifier placed at the mixer output. The cryostat has one helium tank of about 2 liters and one intermediate thermal shield, at a physical temperature of ≈ 20 K, screens the helium tank from external thermal radiations. A block diagram of the receiver is shown in figure 1.

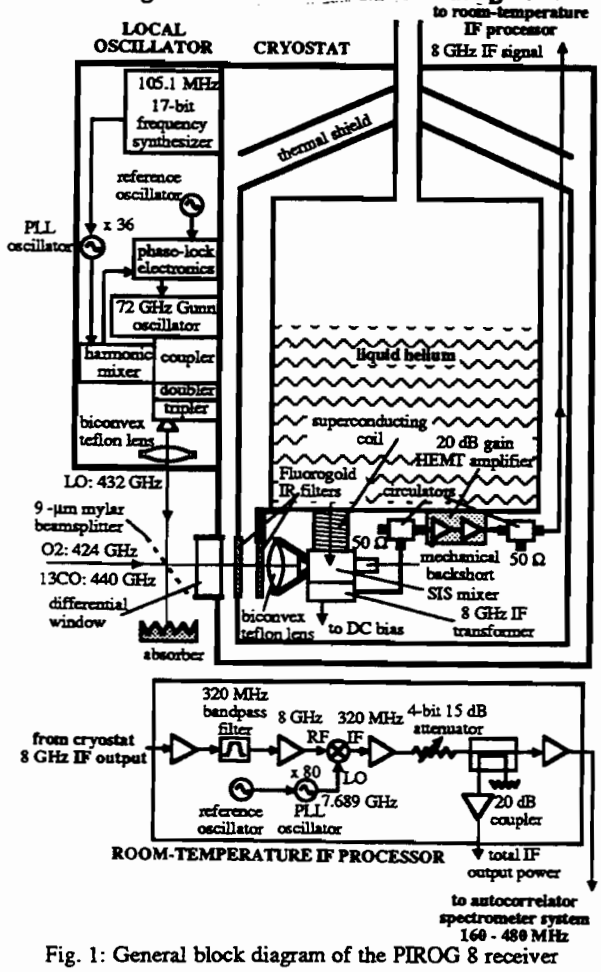

Fig. 1: General block diagram of the PIROG 8 receiver

The signal coming from the secondary mirror of the 60 cm Cassegrain telescope is directly injected in the cryostat through a quartz window with an antireflexion coating. Then it meets a biconvex teflon lens cooled at liquid helium temperature which couples the secondary mirror with the mixer horn. The quasi-optical coupling has been calculated so that the beam-waist is located in the plane of the cryostat window in order to reduce the window size and increase the hold time of the cryostat. Two one-wavelength-thick (450 µm) infrared filters made with fluorogold are installed on the beam path to prevent infrared radiations from heating the mixer. The first one is installed on the intermediate thermal shield at about 20K, the second one is directly fixed in front of the lens and mixer on the stage at liquid helium temperature. A beamsplitter, made with a 9-µm-thick mylar sheet, is located at room-temperature in front of the cryostat window to allow the coupling of a few % of the local oscillator (LO) power in the cryostat. The remaining LO power is absorbed by a submillimeter absorber.

II.2. Controlled phase-locked Local Oscillator

The local oscillator consists of a Gunn oscillator at 72 GHz stabilized in frequency by a dedicated electronics with a phase-lock loop. The frequency of the Gunn output signal is multiplied by 6 by a doubler followed by a frequency tripler[2] in order to generate a few hundreds µW around 433 GHz. The center frequency of the Gunn oscillator is electrically controlled as follows: a 17-bit frequency synthesizer, centered at about 105.3 MHz, tunable from the ground, drives a PLL oscillator at about 3.8 GHz (x 36). The PLL oscillator output signal is injected with a tiny fraction of the Gunn signal in an harmonic mixer. The signal at the intermediate frequency of the harmonic mixer is generated at about 100 MHz by mixing the Gunn signal with the 19th harmonic of the PLL oscillator signal. It is compared with a reference oscillator at 100 MHz by a dedicated electronics which reacts on the Gunn voltage. The phase-lock electronics works over a 600 MHz bandwidth centered at the LO frequency of 433 GHz. This frequency allows the simultaneous detection in the double side-band mode of the O_2 line at 425 GHz and the ^{13}CO line at 441 GHz with a receiver intermediate frequency of 8 GHz. The local oscillator power is also tunable from the ground through the bias voltage of the whisker-contacted varactor diode of the frequency doubler. The local oscillator with its phase-lock electronics is installed on a plate directly fixed on the cryostat in order to simplify and ease the quasi-optical coupling. Moreover, this allows to make the receiver quite compact which is necessary for a balloon-borne experiment where constraints in mass and volume are strong (see figure 1).

II.3. SIS mixer and SIS junction

The mixer uses a 2 μm^2 round-shaped superconducting tunnel junction made in Nb/Al-Al_2O_3/Nb[4]. This junction has a high current density (about 13 kA/cm^2) which corresponds to an $\omega R_N C$ product of 6 at 433 GHz and eases the coupling of the junction with its microwave environment. The associated normal resistance is $R_N = 12\ \Omega$. Moreover, the subgap leakage current is low: the leakage resistance at 2 mV is $R_{sg} = 150\ \Omega$, which corresponds to a ratio $R_{sg}/R_N = 12.5$ and a factor of merit $V_m = 35$.

A tuning circuit[5], using niobium superconducting electrodes, is integrated to the junction in order to resonate out, at the frequency of operation, the high intrinsic capacitance of the junction estimated[6] to 95 $fF/\mu m^2$. The tuning circuit is made of a microstrip line terminated by a 90-degree radial stub and provides, at the frequency of operation, an inductance in parallel with the SIS junction to compensate for its capacitance (see figure 2). The SIS junction, with its integrated tuning circuit, has been fabricated with a low-pass microstrip filter which propagates the mixer output signal at the intermediate frequency of 8 GHz but rejects the mixer input signals at 425, 433 and 441 GHz. All these elements are deposited on a quartz substrate polished at a thickness of 50 µm and diced at the final dimension of 200 µm by 2 mm. The substrate is installed transversally in the waveguide of dimensions 120 by 700 µm.

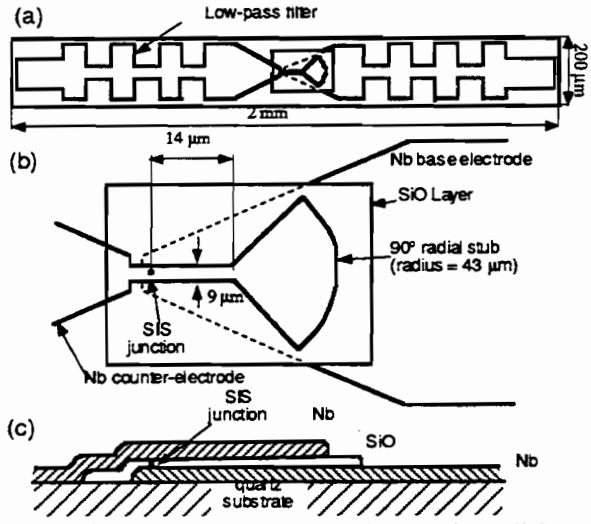

Fig. 2: SIS tunnel junction with an integrated parallel microstrip tuning circuit and low-pass filter. a) general view showing quartz substrate, low-pass filter, SIS junction and tuning circuit. b) Top view showing tuning circuit dimensions. c) Cross section view showing film topology.

The low-pass filter, connected at one end to the mixer ground, is wire-bonded to the input of an impedance transformer at the intermediate frequency. The transformer is realized in microstrip technology on a 1.27 mm-thick Duroïd substrate (relative dielectric constant = 10.2), it is used to transform the mixer output impedance to 50 Ω. It also allows the SIS junction to be DC biased.

On the other hand, a Helmholtz coil, made with niobium-titane superconducting wire, is able to produce a tunable magnetic field in the plane of the SIS junction (up to 1000 Gauss). This is in order to suppress the Josephson currents which add some noise and create instabilities on the receiver. The magnetic field is also tunable from the ground.

II.4. SIS junction fabrication process

The SIS junction has been fabricated[4] by sputtering a trilayer of Nb/Al-Al_2O_3/Nb on a fused quartz substrate. The thickness of the niobium electrodes is about 2000 Å. Then, the low-pass filter is shaped by Reactive Ion Etching of the trilayer in a plasma of SF_6. In a third step, the shape of the junction is defined by photolithography and etched by Reactive Ion Etching in a plasma of SF_6 and O_2. Two gold pads are deposited by evaporation on the ends of the low-pass filter in order to ensure good electrical contacts with the mixer. Then, a 2000 Å-thick SiO layer is evaporated so that the junction perimeter is electrically insulated, this layer is also used as a dielectric for the integrated tuning circuit of the junction. At last, a niobium counter-electrode, which connects the top electrode of the junction to the low-pass filter, is sputtered. This counter-electrode is also used as the top electrode of the integrated tuning circuit.

II.5. Processing of the mixer output signal

The signal coming out of the impedance transformer at the intermediate frequency is amplified by about 20 dB by a low-noise two-stage cryogenic HEMT amplifier located on the cold stage of the cryostat (at the temperature of liquid helium). The average noise temperature of the amplifier is 9 K over a 320 MHz bandwidth centered at 8 GHz. The output signal of the amplifier propagates through a coaxial cable out of the cryostat and is amplified at room-temperature, filtered over a 500 MHz bandwidth and down-converted to the center frequency of the spectrometer, which is 320 MHz. The room-temperature amplification is tunable from the ground from 55 to 70 dB by steps of 1 dB in order to obtain an output level of about -7 dBm, which is the optimal level for the autocorrelator. A telemeasurement of the total output power is also made to control the correct behaviour of the receiver from the ground during the flight and to determine the beam pattern with moon measurements.

II.6. Control electronics

A specific control electronics has been developped to interface the receiver with the gondola electronics. It consists of 5 boards which allow on one hand to telecommand the different modules of the receiver: SIS junction bias voltage, superconducting coil current, HEMT amplifier status (on/off), gain of the room-temperature chain at the intermediate frequency and gain and frequency of the local oscillator.

On the other hand, some telemeasurements are made through this electronics: current and voltage of the SIS junction, total output power, control of the state (on or off) of every module and check of the local oscillator phase-lock status. A portable computer allows to telecommand and control the status of the receiver during the flight.

II.7. Autocorrelator spectrometer

The spectrometer used was an autocorrelator of the hybrid type, and was developed and built at Onsala Space Observatory in Gothenburg for the Astrophysics Division of the European Space Agency. "Hybrid" refers to the fact that the IF band is initially split into several subbands by a set of downconversions using tunable local oscillators. Each subband is then fed to an autocorrelator based on the chip developed[7] by the Netherlands Foundation for Research in Astronomy (NFRA). The maximum bandwidth of the IF is 320 MHz in the range 160-480 MHz; the user may select configurations with bandwidths of 20, 40, 80, 160 and 320 MHz, covered by either 200 or 400 channels. The spectrometer is built into a vessel pressurized with nitrogen gas at 0.5 bar, and cooled by a circulating liquid system. Its mass is around 9 kg, and it consumes about 120 W at peak power. It is controlled by telemetry commands from a dedicated PC (on the ground), which also processes the data from the level of lags up to that of a spectrum.

II.8. Thermal control

Several temperature sensors have been fixed on different subsystems of the receiver to monitor receiver components during flight. Two heating resistors have been installed in order to warm up the receiver if necessary during the balloon ascent when air temperature drops below -50°C.

II.9. Power, volume and mass budgets

The total receiver consumption has been measured to be about 45 watts, the receiver mass, excluding spectrometer, was lower than 28 kg. The front-end is 60 cm high x 23 cm x 30 cm and the electronics boxes overall volume is 19 cm x 18 cm x 18 cm.

III. Ground measurements

III.1. Noise temperature & cryostat hold time

The cryostat hold time has been measured on the ground (T_{helium} = 4.2 K) and was about 20 hours with receiver off and longer than 14 hours with receiver on. A 180 K DSB receiver noise has been measured using the Y-factor technique between room and liquid nitrogen temperatures (see figure 3).

At a helium temperature of 1.5 K, obtained on the ground by pumping on the cryostat helium tank to simulate an external pressure of about 3 mbar, the cryostat hold time was longer than 11.5 hours with ≈ 8.5 hours at ceiling. The best measured DSB receiver noise temperature was 130 K in the laboratory.

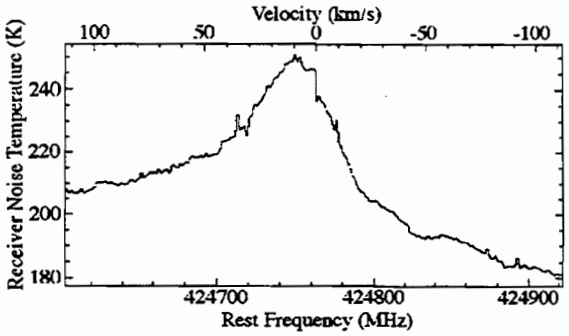

Fig. 3: DSB receiver noise temperature versus lower sideband frequency at 4.2 K helium temperature.

Remark: the variation of the receiver noise temperature in the useful bandwidth, seen in fig. 3, is due to an unfortunate resonance in the impedance transformer at the intermediate frequency, which appears only at low physical temperatures. This does not pose any problem during operation since the lines to observe are located "in the edges" of the bandwidth and take advantage of the lowest receiver noise.

A DSB receiver noise temperature of about 270 K has been measured on the ground before flight. And a noise temperature of about 200 K DSB was expected during flight from the measurements at low pressure (≈ 3 mbars) performed in the laboratory.
Note: The increase of the receiver noise temperature (from about 180 K to 270 K) has been observed in the end of 1996 and is likely due to some slight change of the mixer backshort position caused by repeated thermal cycles between 4 K and room-temperature.

III.2. Sideband ratio

Measurements in the laboratory have shown that the average resonance frequency of the SIS junction with its microwave environment (at which the mixer is supposed to better work) is about

400 GHz, i.e. lower that the normal 433 GHz center frequency of operation.

Some measurements of DC I-V curves pumped at frequencies in the lower and upper mixer sidebands have been performed. The I-V curves have been compared with theoretical predictions based on Tucker's theory in order to determine the mixer gain in each sideband. It appeared that the sensitivity of the mixer is better in the lower side-band where the weak O_2 signal is supposed to be seen. But the sideband gain ratio could not be determined accurately and has been estimated to be between 0.5 dB to 3 dB (gain ratio between 1.1 and 2).

III.3. In-flight calibration setup

A hot and cold load calibration setup has been installed between the telescope and the cryostat to calibrate the receiver in flight. The "cold" load is at ambient temperature and the "hot" load is heated at about 70 °C by a resistor fixed on its backside. Both are made of a submillimeter absorber and can be inserted in the beam path any time during the flight. The low temperature difference (≤ 50 K) between the two loads did not allow us to make accurate noise calibrations but was sufficient to verify the correct behaviour of the receiver. Moreover, ground calibrations showed that the measured hot load temperature had to be decreased by 12 K to account for the "real" receiver noise temperature (measured more accurately with a 77 K liquid nitrogen and a 300 K room temperature set of loads and always used in the past to calibrate the receiver).

III.4. Influence of Josephson currents

One of the main problems encountered with SIS mixers is the presence of Josephson currents[8] in the SIS junction. Also, they depend on the magnetic flux trapped inside the junction. The phenomenom of flux trapping is random and can be provoked by electromagnetic or electrical perturbations. When Josephson currents are present in the junction, some additionnal Josephson noise add to the receiver noise and some instabilities in the output signal make the operation difficult or impossible. Usually, a magnetic field is applied in the plane of the junction in order to suppress the Josephson currents and make the receiver less noisy and more stable. Nevertheless, the currents reappear randomly and the magnetic field needs to be reajusted, which is done on ground or airborne receivers by the operator. In our case, for a balloon-borne experiment, or for some future space applications, this problem becomes overwhelming since there is no operator aboard. It becomes necessary to fully understand the interaction of Josephson currents with the quasiparticle mixing in order to suppress them in a safe way. Consequently, PIROG 8 is a good test bed for such an objective.

Figure 4 displays unpumped and pumped *I-V* curves along with DSB receiver noise temperature versus the SIS junction bias voltage at 4.2 K physical temperature.

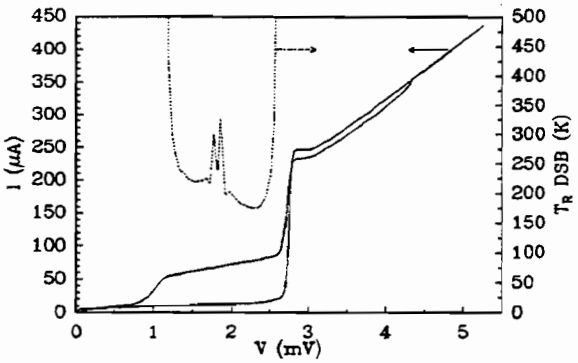

Fig. 4: Unpumped and pumped *I-V* curves and DSB receiver noise temperature versus bias voltage

Though the Josephson currents have been suppressed the best we could by applying the proper magnetic field of about 250 Gauss, one clearly sees that the noise is higher by about 100 K around 1.8 mV. Moreover, the receiver is unstable around this voltage which corresponds to the second Shapiro step at 433 GHz. It turns out that, at 433 GHz, the optimum voltage for lowest receiver noise temperature is about 2.3 mV, i.e. not too close to the Shapiro step. Consequently, the presence of Josephson currents does not hurt too much the operation of the receiver for this particular bias voltage and we observed a very good stability with low receiver noise for more than 8 hours in the laboratory. Nevertheless, the stability depends on the perturbations around the receiver and may be different during the flight due to the different receiver environment (motors, RF transceivers on the gondola, ...)

III.5. Problems with telemetry

Full experiment has exhibited correct behaviour on the ground EXCEPT in presence of real TeleMetry antenna which caused a big perturbation on the front-end and the back-end. Front-end was unstable and could not be operated properly. A few tests with microwave absorbers close to the antenna and with gondola outside the building lead to the conclusion that the receiver should work at ceiling due to the absence of TM power reflected on the experiment.

III.6. Telescope alignment and attitude control

The telescope was aligned with the two TV cameras (a fixed one with a 2° field of view and a movable one with a 0.5° field of view) using a laser and remote light sources. The radioastronomical (RA) focus ('waist') of the telescope was defined using the

optical focus as a reference and then relying on the calculated difference. The optical/radio alignment of the telescope was done using a 30 cm collimator. The set-up was not fully satisfactory and the alignment was judged to be within 2 arcminutes. The RA beam was measured using the 30 cm collimator and it was in agreement with expectations - basically determined by the small size of the collimator (it was planned to use the 1m collimator at Toulouse, but it was occupied by ODIN). The angular position of the sun sensor relative to the telescope was measured using a theodelithe. The software and hardware controlling the azimuth position of the gondola were checked by daytime "observations" of Polaris. The elevation software and hardware were checked by guiding on a star for a couple of hours. The gondola reference horizontal plane deviates from the true one, and two inclinometers are used to measure this deviation. The software is constructed to take care of this effect and this was confirmed by looking at a double star, while tilting the gondola.

IV - Test procedures

Some payload check procedures have been defined during the integration period to verify the correct operation of the receiver, including backend. Some specific routines have been implemented in the software which controls the front-end PC: calibration routines, routines to digitize I-V curves of SIS junctions, routines to use the frequency switch observation mode.

Receiver noise calibrations were performed both by the autocorrelator PC, using power levels measured by the correlator, and the front-end PC, measuring the total output power versus hot and cold loads. Also, a cold against sky calibration routine has been implemented.

Payload check procedures have been defined to verify the correct receiver operation at different frequencies of interest and for different resolutions and bandwidths of the autocorrelator: mainly for observation of O_2 for all scheduled astronomical sources, for observation of ozone lines in order to calibrate the mixer sideband gain ratio, and with frequency offset for sky dip.

Also, routines for frequency switch and position switch modes of observation have been implemented. Several flight simulations have been performed to verify the correct operation of the entire experiment including ground control station and "human interfaces".

V - PIROG 8 flight

V.1. General considerations

The preparations before launch went smoothly, but due to a delay we decided to refill the cryostat in order not to run out of helium in case of a long-duration flight. The launch was smooth.

The duration of the flight was unexpectedly long, leaving 8 hours of observation at ceiling. But, because of repeated TM drop-outs caused by the long distance between gondola and ground base in the end of the flight, the last hour of observations at altitude was essentially lost.

Launch occurred at 5:38 am on september 25th, 1997 from Aire-sur-l'Adour, ceiling was reached at about 8:30 am. Cut-down was decided by CNES at 4:48 pm. Gondola landed in the trees in Massif Central 45 mn after cut-down and was brought back to the base the day after in fairly good conditions.

V.2. Receiver behaviour in flight

The cryostat stayed cold up to the end of the flight. It started to warm up during the descent after cut-down of the balloon. The hold time, higher than 11.5 hours, was a little longer than expected and just enough not to shorten the long flight.

The receiver, front-end and back-end, behaved very well during the entire flight and the fact that it was fully remote-controlled was totally unharmful during the whole flight. Nevertheless a few problems have been observed, fortunately they caused only very minor troubles. First, there has been a few unexpected total power shut-down of the receiver on the ground pad (gondola on batteries) before launch, during the ascent and during the flight when an I-V curve was being digitized. The origin of the shut-down is not known so far but it seems to be correlated with a big number of commands sent to the receiver in a row. Hopefully, the receiver was powered again every time with no damage for the SIS junction.

An expected failure of the phase-lock loop of the synthesized local oscillator happened during the ascent during 1 hour and 40 mn between 10 km altitude (6:20 am local time) and 31 km altitude (08:00 am local time). The outside air temperature was between -40°C and -60°C. The outer shield of the gondola went down to -50°C and the local oscillator plate, which was heated during the ascent, went down to 0°C. The phase-lock stopped functioning below +8°C at 10 km altitude and worked again when it reached +7°C at 31 km altitude. Consequently, the phase-locked system behaved better than expected and made the operation of the receiver possible before reaching ceiling. Figures 5 and 6 show the general temperature variations during flight for different parts of the receiver and gondola. In particular, one can see in figure 6 that heating of the Local Oscillator base plate during ascent has been quite helpful in preventing the phase-lock electronics from cooling down below 0°C, which could have harmed the receiver operation at the beginning of the observations.

At last, the total output power value at the intermediate frequency was corrupted during the same period, very likely by a malfunction of the associated ambient temperature electronics (different gain for operational amplifiers, etc...). It recovered at about 08:15 am local time, again before reaching ceiling.

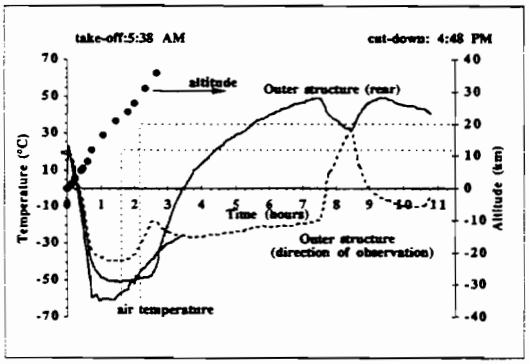

Fig. 5: Temperature variations on different gondola places and altitude profile during PIROG 8 flight.

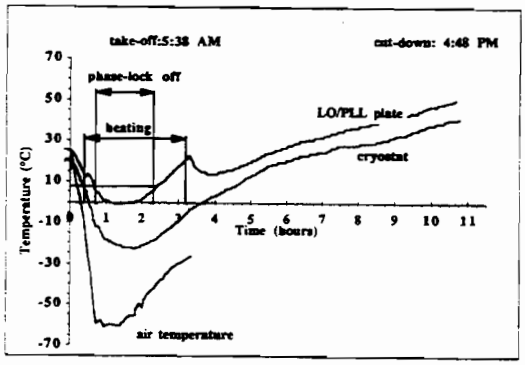

Fig. 6: Temperature variations of receiver components during PIROG 8 flight.

V.3. Stabilizing at altitude

The azimuth stability was achieved as planned and a bright star was quickly found. However, a pendulum motion - not seen in previous flights - was noted. As the inclinometers were useless to trace this motion it could not be compensated for by the control system. We had just to wait for a slow decline. Post-flight analysis with statistical methods of the fine pointing phase shows that pointing was achieved with a RMS value of 0.4 arcminute.

V.4. Alignment

Once the gondola was stabilized, the guide camera was confirmed to be aligned with the fixed camera.

V.5. In-flight receiver calibration

Calibration in flight between sky and ambient calibration load showed that Tr (DSB) was about 295 K. The system DSB noise temperature (including the telescope) was about 500 K. The receiver noise temperature, higher than expected, is likely due to the presence of additional Josephson currents which were hard to suppress. Also, one pumped I-V curve has been digitized at ceiling, it shows that there is a low frequency noise on the SIS junction which smooths the I-V curve non-linearity, hence reducing the performance of the mixer (see figures 7 and 8).. Moreover, this noise, which is likely due to the TM power emitted by the antenna and reflected on the gondola structure, may increase the influence of the remaining Josephson currents and, then, contribute to the lower mixer sensitivity. We had to increase the magnetic field in the plane of the SIS junction to about 500 Gauss during flight, to be compared to 250 Gauss on the ground.

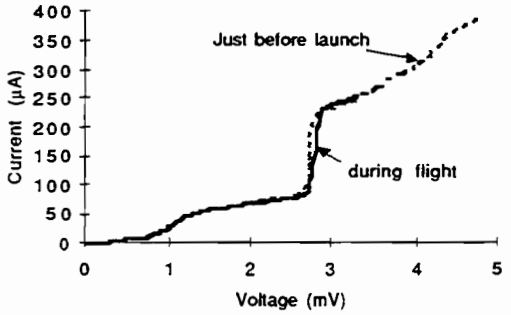

Fig. 7: Experimental pumped I-V curves digitized on ground and during flight.

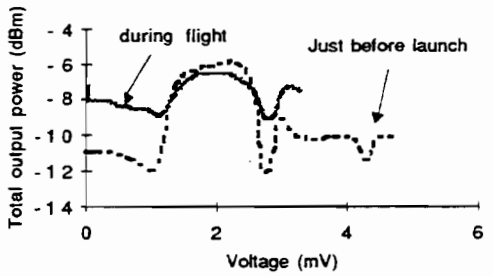

Fig. 8: Experimental output power versus bias voltage curves digitized on ground and during flight. Smoothing of I-V curve is clearly seen. It resulted in degraded performance of the SIS mixer.

V.6. Dip scan.

As planned, the atmospheric emission was measured at a few different elevations. The expected lines were seen, verifying the frequency calibration of the receiver. The dip scan confirms that there is no continuous atmospheric extinction, which means that the low elevation of our main target (down to 18

degrees) does not imply any additional damping of the signal to that given by the telluric O2 line wing.

V.7. Ozone line fit

Another way of measuring the sideband gain ratio in order to improve the accuracy obtained by laboratory measurements has been suggested[9]. It is based on the observation of two atmospheric ozone lines, one in each sideband, for which emission temperatures are known (or at least for which the ratio of their emission temperatures is known). It turns out that the tunability of the local oscillator allows the observations of two ozone lines, respectively centered at about 425.16 and 441.34 GHz. With this technique, the sideband ratio has been estimated to range between 1.2 and 1.25 which is a big improvement compared to the 1.1-2 range obtained in the laboratory. A fit of observations of measured ozone lines at ceiling with theoretical models based on different sideband ratios is shown in figure 9.

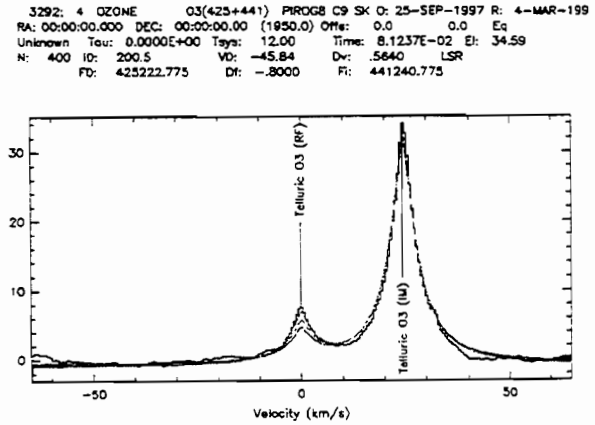

Fig. 9: Experimental spectrum obtained with PIROG 8 receiver at ceiling altitude. Three theoretical fits with different LSB/USB sideband ratios (0.8, 1 and 1.25) are also shown (dashed lines). Best fit is for LSB/USB gain ratio of 1.25

In fact, when the Local Oscillator is tuned to observe the two ozone lines, the ratio is in the range 1.2-1.25 but, once the receiver is tuned at the O2 frequency, the sideband ratio seems to change but we have no direct evidence of this (no O3 line in the upper sideband). Indeed, we need a ratio of 1 to explain the telluric O2 line intensity. The discrepancy may come from the ATM model being not precise enough, from the receiver behaviour itself or from some other reason we could have overlooked. Thus, the overall uncertainty is between 1 and 1.25. It is not due to the method but on the way we can interpret the results in this particular case.

V.8. Calibrations on the moon.

The purpose of the moon observation was to determine the beam efficiency, the beam profile and if possible, to confirm the alignment of radio/optical beams. For some reason - not yet identified - it took a while to find the moon and then in order to gain time, the planned step-by-step scan across the moon was replaced by a few continuous scans, leaving the optical/radio correlation for the post-analysis. The total output power at the intermediate frequency of the receiver has been measured versus moon position. In order to relate the observations with a model, the brightness temperature variation (at 0.7 mm wavelength) across the moon has been derived and convolved with a gaussian beam with a width of 5 arcminutes. The observed data agrees very well with the observations (see figure 10).

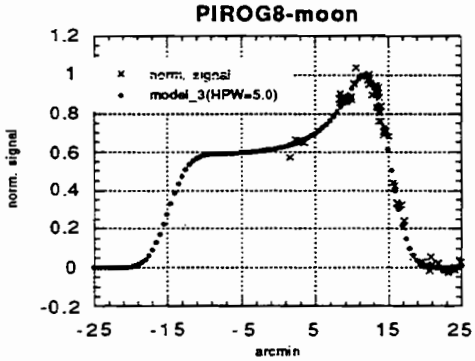

Fig. 10: Experimental and theoretical data of normalized brightness temperature of the moon versus moon position. Date agrees very well with observations.

From this observation, it is also possible to derive the main beam efficiency. If one assumes that the brightness temperature of the hot load is 12 K less than the measured one (as was found on the ground) one calculates a main beam efficiency equal to 0.42. This is slightly lower than our goal (0.6), but in view of our crude ways to align and focus the system, it is not bad. The most probable reason for the low efficiency is that the secondary mirror is a bit over-illuminated (half of the integrated beam from the receiver passing the edge of the mirror). This is in fact not so bad as the sky is transparent and one only sees the cosmic background outside the mirror. This would also mean a slightly lower tapering than usual (10 dB at the edge), which in turn would give a slightly worse side-lobe situation.

VI - Astronomical observations

Two sources have been observed: NGC7538 and W51. A map of the 441 GHz 4-3 13CO line of NGC7538 in the upper sideband has been made. Molecular oxygen has not been detected. Observations will be detailed elsewhere.

Some attempts to observe W51 have been made in the end of the flight but, because of repeated TM drop-outs, the observations were essentially lost. We could, however, confirm the presence of the 13CO line (brighter than in the case of NGC7538), and it may become possible to recover something from the analog recordings of the TM data.

VII. Conclusion

The SIS heterodyne receiver developped for the PIROG 8 balloon project is the first fully remote-controlled submillimeter SIS receiver to have successfully flown on a balloon gondola. It behaved very well during the flight (except for 1 hour and 40 mn during the ascent), which is above expectations. The receiver noise temperature was slightly degraded compared to what was expected from measurements performed on the ground (≈ 300 K instead of 200 K DSB). Some investigations are necessary to safely assess the real causes of this degradation but they seem to be partly due to low-frequency noise in the SIS mixer generated by the TeleMetry antenna.

Project organization - Acknowledgements. PIROG 8 has been developped in the frame of a swedish-french collaboration between the Observatory of Stockholm (PI: Lennart Nordh, Instrument Scientist: Göran Olofsson) and the Observatory of Paris (coPI: Pierre Encrenaz, Instrument Scientist: Laurent Pagani). The project has been managed by Bo Ljung from the Swedish Space Corporation (SSC). The SIS instrument development has been managed by P. Febvre from Paris Observatory. The swedish company ACR was in charge of the gondola and of the interfaces with the receiver. The french space agency (CNES) was in charge of the flight campaign. The Observatory of Paris has developped the instrument with some contributions of the Observatory of Stockholm. The receiver development has been funded by CNES (2/3) and by SSC (1/3). We are very grateful to S. Lebourg and F. Pelletier from Meudon Observatory for their decisive contribution by micromachining the most sensitive parts of this receiver. We also wish to thank J.P. Ayache, V. Thévenet, P. Barroso, J.M. Munier, A. Maestrini and G. Santarelli, from Paris Observatory, for the technical support that they brought to the development of the receiver. Also, we are very grateful to Philippe Goy: indeed, the determination of the sideband ratio in the laboratory has been made possible by using a tunable local oscillator of AB Millimètre.

References

[1] P. Maréchal, Y.P. Viala, and J.J. Benayoun, Astronomy and Astrophysics, vol. 324, pp. 221-236, 1997.

[2] Made by Radiometer Physics, Bergerwiesenstraße 15, 5309 Meckenheim, Germany.

[3] H.M. Pickett, J.C. Hardy, J. Farhoomand, IEEE Trans. Microwave Theory Tech., vol. MTT-32, pp. 936, 1984.

[4] P. Feautrier, M. Hanus and P. Febvre, Supercond. Sci. Technol., vol. 5, pp. 564-568, 1992.

[5] P. Febvre, C. Boutez, S. George and G. Beaudin, Proceedings of the International Conference on Millimeter and Submillimeter Waves and Applications II, vol. SPIE 2558, pp. 136-147, San Diego Convention Center, 9-14 July 1995.

[6] P. Febvre, W.R. McGrath, P. Batelaan, B. Bumble, H.G. LeDuc, S. George, P. Feautrier, International Journal of Infrared and Millimeter Waves, vol. 15, no. 6, pp. 943-965, June 1994.

[7] A. Bos, "The NFRA correlator chip", NFRA ITR 176, 1986.

[8] B.D. Josephson, Phys. Lett., vol. 1, pp.251-253, July 1962.

[9] Jose Cernicharo (private communication).